

# The Keystone Transformation for Correcting Range Migration in Range-Doppler Processing

Mark A. Richards

March 2014

## 1 Acknowledgement

Thanks to Dr. Gregory Showman of the Georgia Tech Research Institute for helping me to understand this topic with his usual lucid explanations. The keystone transformation for compensating range migration is discussed in a number of papers, e.g. [1],[2].

## 2 The Problem

Conventional range-Doppler (RD) processing collects a coherent processing interval (CPI) of fast-time/slow-time data ("ft" and "st") and performs a slow-time discrete Fourier transform (DFT) on all range bins to convert it to an RD matrix. Implicit is the assumption that the target velocity  $v$ , CPI duration  $T_a$ , and range bin spacing  $\delta R$  are such that the target's range change within the CPI is less than one range bin,  $vT_a < \delta R$ . In other words, the target stays in the same range bin over the duration of the CPI. If this is the case, all of the target signature will be in the same range bin and a 1D slow-time DFT will result in a well-formed, full-resolution Doppler spectrum. For a constant-velocity target without slow-time windowing, this spectrum will be just an asinc<sup>1</sup> function in the Doppler coordinate with a Rayleigh width of approximately  $1/T_a$  Hz (assuming no windowing for sidelobe control). Figure 1a is a diagram of a notional data matrix in which the target stays in the same (gray-shaded) range bin over the CPI.

这里是CPI时间间隔，例如  
PRT=132e-6，发射  
1024个就是  
1024PRT = CPI

如果速度固定，相当于  
一个点频加了矩形窗，  
是sinc函数频谱搬移

A simulated range-Doppler matrix was generated by modeling a target in range bin #100 that approaches the radar at 20 m/s. It is assumed that waveform and matched filtering used are such that the range response of the radar is an unwindowed sinc function with a Rayleigh resolution of  $\Delta R = c/2B$  m. The radar frequency is  $F_0 = 10$  GHz and its bandwidth is  $B = 200$  MHz, giving  $\Delta R = 0.75$  m. However, the fast-time axis is oversampled by a factor of 2.3x, so the spacing of the range bins is  $\delta R = 0.3261$  m. The CPI is  $M = 101$  pulses long at a PRF of 10 kHz, giving a CPI duration of  $T_a = 10.1$  ms. In this time, the target moves 0.202 m or 0.62 range bins. The target velocity corresponds to a Doppler shift of  $F_D = 13.33$  kHz and an unaliased normalized Doppler shift of  $f_D = +0.133$  cycles/sample. Note that the range-Doppler spectrum peak does occur at  $l = 100$  and  $f_D = 0.133$ .

距离单元和速度单元

<sup>1</sup> "aliased sinc" function, also sometimes called a "digital sinc" (dsinc) or Dirichlet function [3].

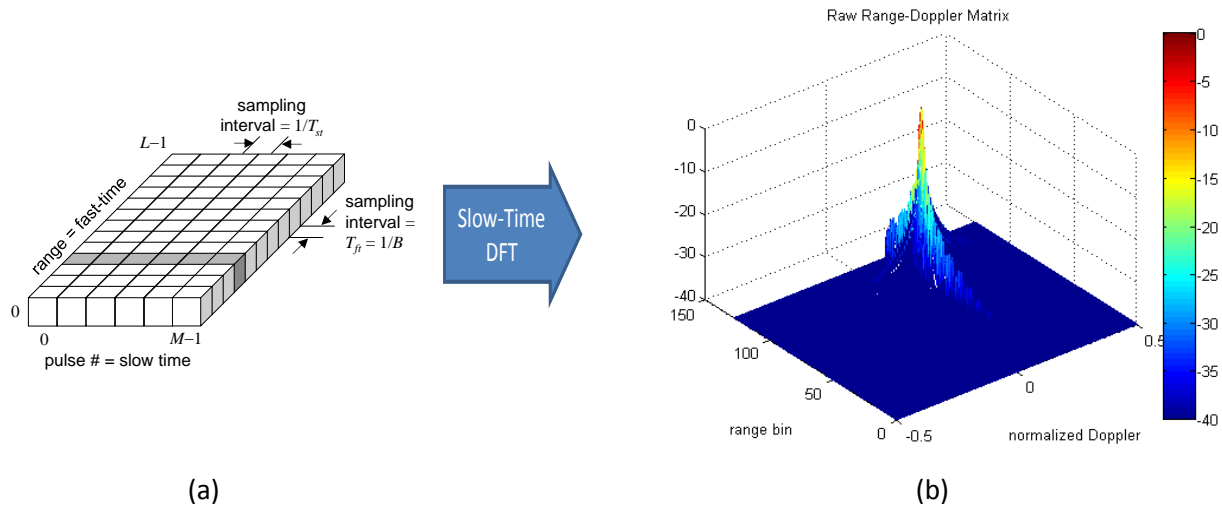


Figure 1. Range-Doppler matrix for a single target without range migration. (a) Arrangement of fast-time/slow-time data. (b) Resulting range-Doppler matrix. See text for parameters.

When the target does not remain within a single range bin over the CPI, *range migration* is said to occur. The target Doppler signature will smear in both range and Doppler. It smears in range because portions of the target signature appear in more than one range bin. It smears in Doppler because any one range bin contains the signature for only a portion of the CPI. Since Doppler resolution (width of the asinc mainlobe) in a given range bin is inversely proportional to signal duration in that range bin, the reduced duration degrades the Doppler resolution (broadens the mainlobe). Range migration is obviously more severe for fast-moving targets. However, it is also made worse in wide-bandwidth systems. Such systems have fine range resolution and therefore smaller spacing between range bins, so that a given amount of motion crosses more bins.

Consider an  $L \times M$  ft/st matrix  $y_{rd}[l, m]$ .<sup>2</sup> Suppose a radar transmits a series of  $M = 2M_a + 1$  pulses which reflect from a target. The slow-time sampling interval (the radar PRI) is  $T_{st}$  seconds. Assume the slow-time span of the CPI is from  $-T_a/2 = -M_a T_{st}$  to  $+T_a/2 = +M_a T_{st}$ , so that the center of the CPI is at time  $t = 0$  and pulse  $M = 0$ . Note that the unambiguous Doppler range is  $\pm 1/2T_{st}$  Hz.

If the fast-time sampling interval is  $T_{ft}$  seconds, the range bin spacing is  $\delta R = cT_{ft}/2$  meters. It is usually the case that  $T_{ft} \approx 1/B$ , where  $B$  is the instantaneous bandwidth of the radar waveform; but we do not require this. Assume the range corresponding to the first range bin ( $l = 0$ ) is  $R_0$ . Express the target range

<sup>2</sup> A lower case  $r$  or  $d$  in the subscript to a signal  $y$  or  $Y$  indicates a signal in the time domain in the corresponding dimension. An upper case  $R$  or  $D$  indicates that the signal is in the frequency domain in that dimension. An upper case  $Y$  is used when at least one of the dimensions is in the frequency domain. Thus  $y_{rd}$  is raw fast time/slow time data, while  $Y_{rD}$  is a function of fast time and Doppler frequency, i.e. the range-Doppler matrix. Square brackets indicate discrete variables, parentheses indicate continuous variables.

$R_{ref}$  at the center of the CPI as  $R_{ref} = R_0 + R_{rel}$ , i.e.  $R_{rel}$  is the reference range relative to  $R_0$ . Let the range bin corresponding to  $R_{rel}$  be  $l_{rel}$ . Thus,  $l_{rel} = (2R_{rel}/c)/T_{ft} = R_{rel}/\delta R$ .

The target radial velocity relative to the radar is  $v$  m/s, with positive  $v$  representing approaching targets. The target range on the  $m^{\text{th}}$  pulse ( $-M_a \leq m \leq M_a$ ) will be  $R_{ref} - vT_{st}m = R_0 + R_{rel} - vT_{st}m$ , corresponding to range bin  $l_{rel} - 2vT_{st}m/cT_{ft} = l_{rel} - vT_{st}m/\delta R$ . (The range bin number is rounded to the nearest integer.)

Assume the RF is  $F_0$  Hz. The radar transmits a pulse of the form  $\bar{x}(t) = x(t)\exp(j2\pi F_0 t)$ , where  $x(t)$  is the baseband waveform (for example, a simple pulse or LFM chirp, etc.). After taking out the delay of  $mT_{st}$  to the beginning of that pulse's transmission and demodulation to baseband by multiplication with the function  $\exp(-j2\pi F_0 t)$  to remove the carrier, the received fast-time signal for the  $m^{\text{th}}$  pulse will be of the form [3]

$$y_m(t) = x\left(t - \frac{2}{c}(R_{ref} - vT_{st}m)\right) \exp\left[-j\frac{4\pi F_0}{c}(R_{ref} - vT_{st}m)\right] \quad (1)$$

$$= x\left(t - \frac{2}{c}(R_{ref} - vT_{st}m)\right) \exp\left(-j\frac{4\pi F_0}{c}R_{ref}\right) \exp\left(+j\frac{4\pi F_0}{c}vT_{st}m\right)$$

其实这种形式好理解，就是瞬态位置固定后的回波相对复相位  
 $\exp(-j \cdot 2 \cdot \pi / \lambda \cdot (2R - 2\delta l \cdot \text{taR}))$

这个是多普勒项

这个是时延项

这个就是随便一个空间点相位的参考

Amplitude factors are of no concern here and so have been ignored.

Now assume this baseband signal is passed through the matched filter for the envelope  $x(t)$ . Regardless of the particular waveform the matched filter output (after removing the matched filter delay) can be modeled as consisting of a dominant peak of Rayleigh width approximately  $1/B$  seconds at the appropriate time delay, surrounded by low-amplitude sidelobes. For this analysis, a sinc function in fast time with a zero spacing of  $1/B$  seconds, i.e.  $x(t) = \sin(\pi Bt)/(\pi Bt) \equiv \text{sinc}(Bt)$ , has been selected to represent a typical matched filter output.<sup>3</sup> The demodulated and matched-filtered output becomes

$$y_m(t) \approx \exp\left(-j\frac{4\pi F_0}{c}R_{ref}\right) \exp\left(+j\frac{4\pi F_0}{c}vT_{st}m\right) \text{sinc}\left(B\left(t - \frac{2}{c}(R_{ref} - vT_{st}m)\right)\right) \quad (2)$$

This analog data is converted to discrete fast-time data by sampling at the range bin interval of  $T_{ft}$  seconds. Sampling begins at the time delay corresponding to  $R_0$ , so samples are taken at times  $t = 2R_0/c + l \cdot T_{ft}$ ,  $l = 0, \dots, L-1$ . The resulting fast-time vector is

<sup>3</sup> The definition  $\text{sinc}(x) = \sin(\pi x)/\pi x$  is consistent with that used in both MATLAB® and [3].

$$\begin{aligned}
 y_m[l] &\approx \exp\left(-j\frac{4\pi F_0}{c}R_{ref}\right)\exp\left(+j\frac{4\pi F_0}{c}vT_{st}m\right)\text{sinc}\left(B\left(T_{ft}l - \frac{2}{c}(R_{rel} - vT_{st}m)\right)\right) \\
 &= \exp\left(-j\frac{4\pi F_0}{c}R_{ref}\right)\exp\left(+j\frac{4\pi F_0}{c}vT_{st}m\right)\text{sinc}\left(BT_{ft}\left(l - \frac{2}{cT_{ft}}R_{rel} + \frac{2vT_{st}}{cT_{ft}}m\right)\right) \\
 &= \exp\left(-j\frac{4\pi F_0}{c}R_{ref}\right)\exp\left(+j\frac{4\pi F_0}{c}vT_{st}m\right)\text{sinc}\left(BT_{ft}\left(l - l_{rel} + \frac{vT_{st}}{\delta R}m\right)\right)
 \end{aligned} \tag{3}$$

The returns from each of the  $M$  pulses in the CPI are assembled into the raw fast-time/slow-time matrix  $y_{rd}[l,m]$ :

$$y_{rd}[l,m] \approx \exp\left(-j\frac{4\pi F_0}{c}R_{ref}\right)\exp\left(+j\frac{4\pi F_0}{c}vT_{st}m\right)\text{sinc}\left(BT_{ft}(l - l_{rel} + l_m)\right) \tag{4}$$

where  $l_m = vT_{st}m/\delta R$ . Note that  $l_m$  is not integer in general.

**Figure 2a** illustrates the pattern of data corresponding to Eq. (4) for the same case used in Fig. 1. Again, the simulation was carried out for  $L = 128$  range bins and  $M = 101$  pulses. The normalized Doppler shift is  $f_D = F_D T_{st} = (2vF_0/c)T_{st} = 0.133$  cycles/sample. There is no significant range migration (0.62 range bins over the CPI) from the reference range bin of  $l_{rel} = 100$  at the center of the CPI. Figure 2a shows the magnitude of the range bin vs. pulse number (fast time/slow time) data, illustrating that the signal peak stays within range bin #100. The oversampling factor of  $2.3\times$  in fast time makes it possible to see some of the sidelobe structure of the sinc response in fast time. **Figure 2b** shows the central portion of the resulting range-Doppler spectrum. The white dotted lines mark the reference range bin at the middle of the CPI ( $l_{rel} = 100$ ) and normalized Doppler shift ( $f_D = 0.133$ ) of the spectrum, and thus the expected spectrum peak location. The white square shows the expected Rayleigh resolution extent (expected location of first null) in each dimension. In the absence of range migration, the spectrum is a clean two-dimensional sinc/asinc with its peak at the correct location and full resolution in both range and Doppler.

**Figure 3** shows a similar example, with two changes. The target velocity is now 440 m/s, giving a significant range migration of 13.63 bins over the CPI. The RF frequency has been reduced to  $F_0 = 1$  GHz, making the Doppler shift  $F_D = 2.933$  kHz and the normalized Doppler frequency now  $f_D = 0.2933$  cycles/sample. The reduction in  $F_0$  allows for an unaliased Doppler at this velocity; see Section 6. It is clear that the signature is spread over a little more than 13 range bins and that its mainlobe in the Doppler dimension, while correctly centered, has also been severely broadened.

Matlab 仿真:  
keystone.m

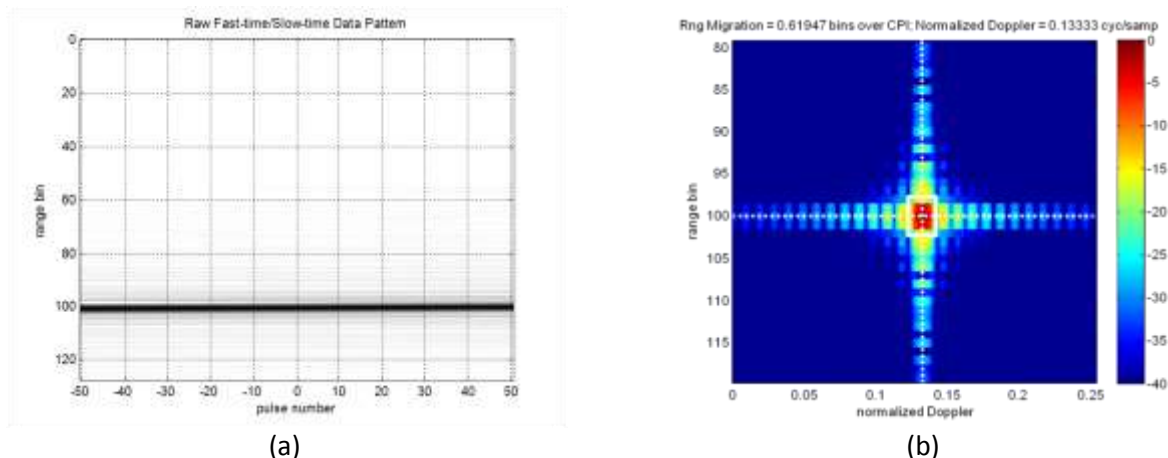


Figure 2. Range-Doppler matrix with no range migration. (a) Range vs. pulse number. (b) Zoom into the central portion of the resulting range-Doppler matrix.

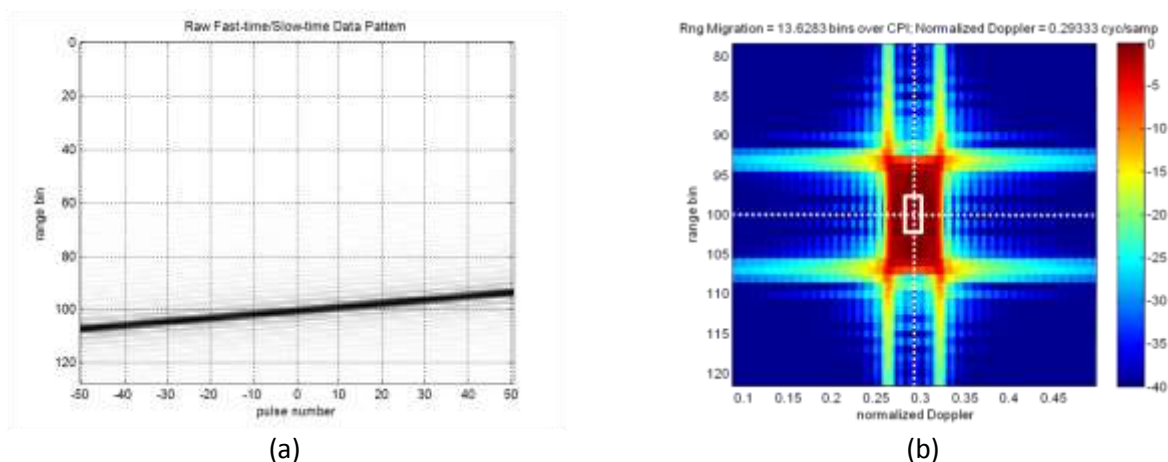


Figure 3. Range-Doppler matrix with range migration. Compare to Fig. 2. (a) Range vs. pulse number. (b) Zoom into non-zero portion of the resulting range-Doppler matrix.

### 3 Compensation by Range Shifting

The goal of the keystone transformation is to develop a process that will compensate for the range migration so that the range-Doppler spectrum of the data in Fig. 3a looks like Fig. 2b instead of Fig. 3b. To begin, consider compensating for range migration in the not-very-useful case of a single target with known radial velocity. The target moves  $vT_{\text{sr}}/\delta R$  **range bins** closer to the radar on each successive pulse. This is easily corrected by shifting each successive fast-time vector by  $-vT_{\text{sr}}/\delta R$  bins with respect to the previous pulse data. The reference range to which all echoes will be shifted can be chosen arbitrarily. One obvious choice is the range  $R_{\text{ref}}$  (equivalently,  $R_{\text{rel}}$  relative to the first range bin at  $R_0$ ) at the middle of the CPI.

The range can be shifted using properties of the discrete-time Fourier transform (DTFT). Recall that  $y_m[l]$  is the fast-time data for the  $m^{\text{th}}$  pulse given in Eq. (3), and let  $Y_m(\omega_l)$  be its DTFT. Then standard DTFT properties state that

$$\mathbf{F}^{-1} \{ \exp(-j\omega_l l_m) Y_m(\omega_l) \} = y_m[l - l_m] \equiv y'_m[l] \quad (5)$$

通过傅里叶变换的复数指数项来距离补偿

where  $\mathbf{F}^{-1}\{\cdot\}$  represents the inverse DTFT (IDTFT). Because the desired shift  $l_m = vT_{st}m/\delta R$  is not integer in general, the quantity  $y_m[l - l_m]$  means the corresponding shifted analog signal  $y_m(t - (vT_{st}/\delta R)m)$  sampled at the times  $T_{st}l$ .

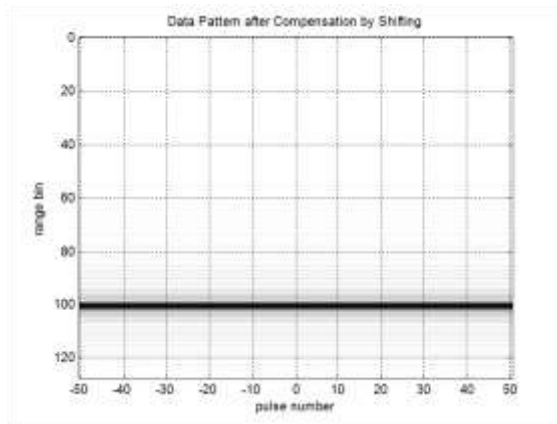
The shift is applied in practice by first computing the  $K_l$ -point DFT  $Y_m[k_l]$  of the fast time data, performing an "fft shift" operation to circularly shift the resulting vector of  $K_l$  DFT samples so that the sample corresponding to  $k_l = 0$  (and thus to  $\omega_l = 0$ ) is **in the center of the vector**. The DFT size  $K_l$  must be greater than or equal to the number of range bins,  $L$ . The shifted DFT is then multiplied by the phase function of Eq. (5). The modified DFT is circularly rotated back to its original order,<sup>4</sup> and finally an inverse DFT is computed to obtain  $y'_m[l]$ . The inverse DFT returns a  $K_l$ -point fast-time sequence; only the first  $L$  points are retained.

fft点数必须比采样点数多

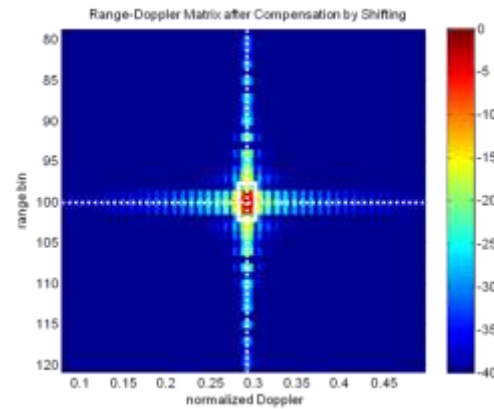
乘以一个复数项让他自己在复数平面旋转，然后还原

逆变换虽然是fft点数这么多，但是我们只取采样点来表示，因为只有这部分是有效的

Figure 4 illustrates the result of applying this compensation procedure to the data of Fig. 3a. The results are excellent: the target signature data is re-centered into range bin 100 for all pulses, resulting in a range-Doppler spectrum with the full expected resolution in both dimensions. The spectrum shape is nearly indistinguishable in shape from that of the negligible-migration case of Fig. 2, except for being centered at a different Doppler value in accordance with the change in velocity.



(a)



(b)

**Figure 4. Range-Doppler matrix with range migration and compensation using DFT phase multiplies. Compare to the spectrum shape in Figs. 2 and 3. (a) Range vs. pulse number. (b) Zoom into non-zero portion of the resulting range-Doppler matrix.**

<sup>4</sup> The MATLAB® functions `fftshift` and `ifftshift` implement the required rotations.

While the results in Fig. 4 are very good, they require two assumptions, both problematic:

1. The target velocity  $v$  is known. This is required to compute the DFT phase modification function in Eq. (5). Knowledge of  $v$  implies that the target is already under track or that other sensors or information sources provide this information. Alternatively, the data can be processed with a series of different trial values of  $v$  in an attempt to identify the velocity by finding the value that best "focuses" the spectrum, usually interpreted as that value that provides the largest peak. If the target velocity might be aliased, it may also be necessary to estimate both the aliased velocity and the ambiguity number (number of foldovers); see Section 6.
2. There is only one target (or all targets have the same radial velocity). Otherwise, there is more than one value of  $v$  to be corrected, so there is no single DFT phase modification function that can be used.

Notice that if there were only a single target with a known velocity, the range migration could also be compensated by simply adjusting the start of the fast-time sampling times for each successive pulse so that the target remained at a constant delay relative to the transmission time for the current pulse.

## 4 The Keystone transformation

A more robust range migration compensation method can be developed as follows. First let us establish the goal, which is to obtain the range-Doppler spectrum of Fig. 4b corresponding to a target at relative range  $R_{ref}$  and normalized Doppler shift  $f_D$ , with full resolution in both dimensions as determined by the waveform bandwidth  $B$  and CPI duration (aperture time)  $T_a$ . It is convenient to work with continuous fast time  $t$  instead of sampled fast time  $l$ . In the fast time (range) dimension the desired response is, to within a complex constant,  $\text{sinc}\left[B(t - 2R_{ref}/c)\right]$ . The fast-time Fourier transform (FT) of this function would have unit magnitude over the fast-time baseband frequency interval  $F \in [-B/2, B/2]$  and zero elsewhere, and a phase of  $\exp\left[-j2\pi F(2R_{ref}/c)\right] = \exp(-j4\pi R_{ref}F/c)$  within that interval. This would be the same for each pulse (value of  $m$ ) because there would be no range migration. In the cross-range dimension, the desired Doppler spectrum is the DTFT of a constant-frequency discrete-time sinusoid at the Doppler frequency  $2vF_0/c$ , sampled at the interval  $T_{st}$ . The corresponding slow-time phase progression is the sequence  $\exp(j2\pi(2vF_0/c)T_{st}m) = \exp(j4\pi vT_{st}(F_0/c)m)$ . Combining the fast- and slow-time data patterns gives the ideal two-dimensional fast time/slow time data function

$$y_{rd\_ideal}(t, m) = \exp\left(-j\frac{4\pi}{c}F_0R_{ref}\right) \exp\left(+j\frac{4\pi}{c}F_0vT_{st}m\right) \text{sinc}\left(B\left(t - \frac{2}{c}R_{ref}\right)\right) \quad (6)$$

Now form the two-dimensional function  $Y_{Rd\_ideal}(F, m)$  by computing the FT of  $y_{rd\_ideal}(t, m)$  in fast time. The result will be



$$Y_{Rd\_ideal}(F, m) = \begin{cases} \exp\left(-j\frac{4\pi}{c}(F + F_0)R_{ref}\right) \exp\left(+j\frac{4\pi}{c}F_0vT_{st}m\right), & -B/2 < F < +B/2, \\ & -M_a < m < +M_a \\ 0, & \text{otherwise} \end{cases} \quad (7)$$

Notice that the fast-time baseband **frequency  $F$  and the velocity  $v$  are uncoupled**, that is, they appear in separable terms. If the fast-time Fourier transform of the **actual data  $y_{rd}(t, m)$**  can be manipulated to be in the form of Eq. (7), the corresponding range-Doppler spectrum will be correctly centered and well-focused in both dimensions.

To that end, now consider the **Fourier transform of the actual fast-time signal of Eq. (2)**. Using arguments similar to those leading to Eq.(7) gives

$$\begin{aligned} \mathbf{F}\{y_m(t)\} &\approx \exp\left(-j\frac{4\pi F_0}{c}R_{ref}\right) \exp\left(+j\frac{4\pi F_0}{c}vT_{st}m\right) \exp\left[-j2\pi F\left(\frac{2}{c}(R_{ref} - vT_{st}m)\right)\right] \\ &= \exp\left(-j\frac{4\pi}{c}(F_0 + F)R_{ref}\right) \exp\left(+j\frac{4\pi}{c}(F_0 + F)vT_{st}m\right), & -B/2 < F < +B/2, \\ &\equiv Y_{Rd}(F, m) & -M_a < m < +M_a \end{aligned} \quad (8)$$

等于这里面多了一个F项

所以当F>0的时候比预期的多普勒高

F<0比预期的多普勒低，这样子多普勒估计就和信号的带宽耦合了

We see that **the fast-time frequency and velocity** are not separable in this expression, but instead are coupled in the slow-time phase term (the second **exponential phase term**). At frequencies greater than  $F_0$  ( $F > 0$ ) the sample-to-sample slow-time phase progression rate is faster than the desired value of  $F_0vT_{st}$ , while at frequencies lower than  $F_0$  ( $F < 0$ ) it is slower than desired.

Equation (8) is the model for the structure of the fast-time FT  $Y_{Rd}(F, m)$  of the available measured data matrix  $y_{rd}(t, m)$ . We now seek an operation on  $Y_{Rd}(F, m)$  that will **transform it to the desired form**  $Y_{Rd\_ideal}(F, m)$  of Eq. (7), to within a constant. An obvious approach is to multiply  $Y_{Rd}(F, m)$  by the phase term  **$\exp(-j(4\pi/c)FvT_{st}m)$** . However, this technique has the same flaws (and in fact is identical to) the range-shifting method of the previous section: one would have to know  $v$  and the process would only work for one target.

A clever way to **remove the frequency-velocity coupling proceeds as follows**. Concentrate on the slow-time term, since that is where the coupling occurs.  $Y_{Rd}(F, m)$  is sampled in slow time at the times  $\tau_m = m \cdot T_{st}$ ,  $-M_a \leq m \leq M_a$  where  $M = 2M_a + 1$ . It is convenient to rewrite  $Y_{Rd}(F, m)$  in terms of a continuous slow-time variable  $\tau$ :

$$Y_{Rd}(F, \tau) = \exp\left(-j\frac{4\pi}{c}(F_0 + F)R_{ref}\right) \exp\left(+j\frac{4\pi}{c}(F_0 + F)v\tau\right), \quad \begin{matrix} -B/2 < F < +B/2, \\ -M_a T_{st} < \tau < +M_a T_{st} \end{matrix} \quad (9)$$

Define **a new slow-time variable** that rescales the slow-time axis as a function of fast-time frequency according to



$$\tau' = \left( \frac{F_0 + F}{F_0} \right) \tau \Rightarrow \tau \equiv \left( \frac{F_0}{F_0 + F} \right) \tau' \quad (10)$$

At  $F = 0$  the slow-time dimension is unchanged. For  $F > 0$  it is expanded in slow time ( $\tau' > \tau$ ), while for  $F < 0$  it is contracted ( $\tau' < \tau$ ). For  $F > 0$  this will have the effect of stretching the sample-to-sample phase progression over a longer time interval, thus reducing the time rate of phase change and therefore the slow-time frequency. For  $F < 0$  the slow-time frequency will be increased in the rescaled data.

Substituting from Eq. (10) for  $\tau$  in Eq. (8) gives the new function

$$\begin{aligned} Y_{Rd\_key}(F, \tau') &\equiv Y_{Rd} \left( F, \left( \frac{F_0}{F_0 + F} \right) \tau' \right) \\ &= \exp \left( -j \frac{4\pi}{c} (F_0 + F) R_{ref} \right) \exp \left( +j \frac{4\pi}{c} (F_0 + F) v \left( \frac{F_0}{F_0 + F} \right) \tau' \right) \\ &= \exp \left( -j \frac{4\pi}{c} (F_0 + F) R_{ref} \right) \exp \left( +j \frac{4\pi}{c} v F_0 \tau' \right) \\ &= Y_{Rd\_ideal}(F, \tau') \end{aligned} \quad (11)$$

Equation (11) is the desired result. It shows that a fast-time FT and a slow-time rescaling according to Eq. (10) will result in a new function that is the fast-time FT/slow-time inverse FT of the desired range-Doppler spectrum. An inverse FT in the range dimension and a forward FT in the pulse number dimension will result in the focused range-Doppler image with no degradation in either range or Doppler due to range migration.

The rescaling of Eq. (10) implies one-dimensional interpolation of the sampled slow-time data in each fast-time frequency bin. The interpolation factor varies with fast-time frequency. Specifically, constant sampling intervals of  $T_{st}$  in  $\tau'$ ,  $\tau'_m = T_{st} m$ , require values of the original data  $Y_{Rd}(F, \tau)$  at the points  $\tau_m = (F_0 / (F_0 + F)) \tau'_m = (F_0 / (F_0 + F)) T_{st} m$ . An appropriate approach is bandlimited interpolation using sinc-based interpolation kernels [4], though simpler methods such as spline interpolation might be adequate in some cases. ← 重要, sinc插值方法

The region of support (ROS) of  $Y_{Rd\_key}(F, \tau')$  in fast-time frequency is the same as that of the original data  $Y_{Rd}(F, \tau)$ , namely  $(-B/2, +B/2)$ . The ROS in slow-time varies with fast-time frequency. The original slow-time variable  $\tau$  is confined to the interval  $(-M_a T_{st}, +M_a T_{st})$ . The range of the new slow-time variable  $\tau'$  is therefore

$$-\left( \frac{F_0 + F}{F_0} \right) M_a T_{st} \leq \tau' \leq +\left( \frac{F_0 + F}{F_0} \right) M_a T_{st} \quad (12)$$

This implies that the range of the slow-time index  $m$  in the transformed data will be

$$\left[ -\left( \frac{F_0 + F}{F_0} \right) M_a \right] \leq m \leq \left[ +\left( \frac{F_0 + F}{F_0} \right) M_a \right] \quad (13)$$

The floor and ceiling functions are needed to restrict  $m$  to an integer range. For  $F < 0$  this range will be less than the original full range of  $-M_a \leq m \leq M_a$ . For  $F > 0$  Eq. (13) states that the range should be greater than  $\pm M_a$ . In practice, however, the range is limited to  $\pm M_a$  because there is no data to support interpolation into a larger range.

Figure 5 illustrates the results of applying the keystone transformation to the same scenario used for Fig. 3. A Hamming-windowed bandlimited sinc interpolating filter was used to interpolate  $Y_{Rd}(F, \tau)$  in slow time. The filter length was 11 times the maximum of the slow-time sample spacing before and after interpolation;<sup>5</sup> the specific value varies with fast-time frequency because of the variation in the interpolation factor  $F_0/(F_0+F)$ . Note in Fig. 5a that the range migration has been removed. The fading and fast-time smearing of the ft/st signature at the beginning and end of the CPI is due to end effects of the interpolation: the first and last few slow-time samples cannot be fully interpolated because the interpolation filter impulse response extends beyond the ends of the available data. This will result in a slight loss of Doppler resolution that will become more severe for longer interpolation filters. Figure 5b shows the resulting range-Doppler spectrum. The peak is correctly centered and obtains very nearly full resolution in both dimensions. Some modification of the sidelobe structure is evident in the "X-shaped" Doppler sidelobes, but this is of little consequence and can be reduced by windowing.

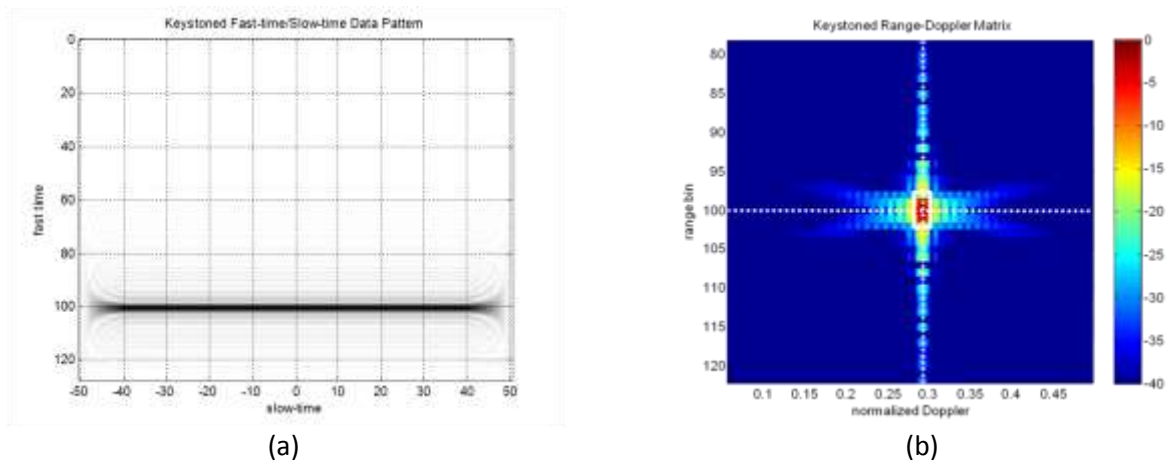


**Figure 5. Range-Doppler matrix with range migration and compensation using the keystone transformation. Compare to Figs. 3 and 4. (a) Range vs. pulse number. (b) Zoom into non-zero portion of the resulting range-Doppler matrix.**

<sup>5</sup> See the MATLAB® code for the function `sinc_interp` included at the end of this memo for details.

A major advantage of the keystone transformation for range migration correction over the shifting process discussed earlier is that **it correctly handles multiple targets**. Notice that the rescaling of Eq. (10) does not depend on target velocity  $v$ . Consequently, target velocity need not be known, and this process will simultaneously correct range migration for multiple targets of various velocities. Figure 6 illustrates this with another example using three targets having (reference range bin, velocity (m/s)) pairs of (30, -200), (60, 0), and (65, 650). All radar parameters are unchanged. The resulting range migrations over the CPI are -6.1947, 0, and +20.1327 bins, while the normalized Doppler shifts are -0.1333, 0, and +0.4333 cycles/sample. Figure 6 illustrates the results. Part (a) of the figure shows the ft/st data pattern. Note that two of the targets cross during the CPI. Figure 6b shows the range-Doppler spectrum before the keystone transformation. The zero-velocity (non-migrating) target is well-focused; the other two are not, with the degree of defocus increasing at higher velocities (more range migration).

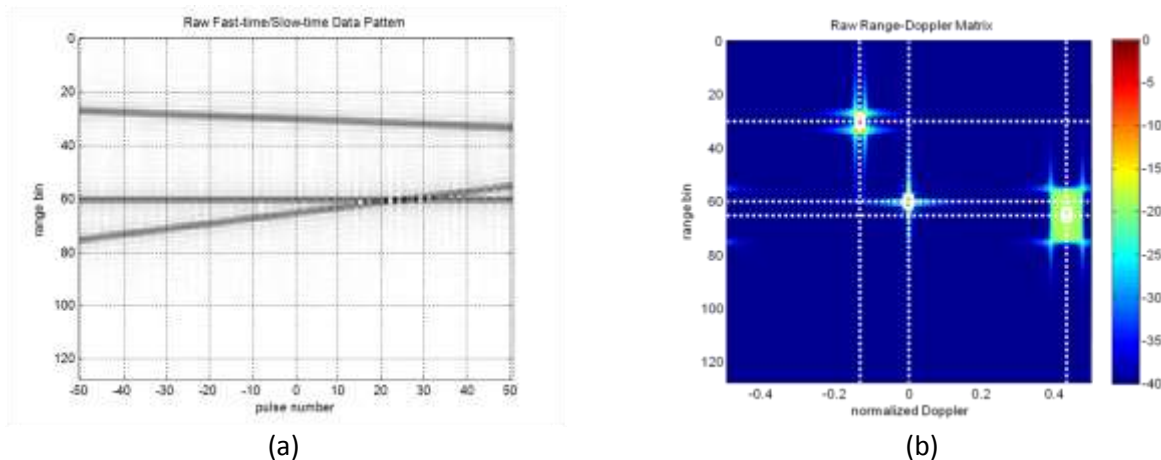


**Figure 6. Range-Doppler matrix with multiple targets at different velocities. (a) Range vs. pulse number. (b) Zoom into non-zero portion of the resulting range-Doppler matrix.**

Figure 7 shows the results of applying the keystone transformation to this example. Figure 7a shows that each target's signature has been realigned to a single range bin. Figure 7b shows the resulting range-Doppler spectrum, now having nearly full resolution in both dimensions on all three targets, despite their differing velocities.

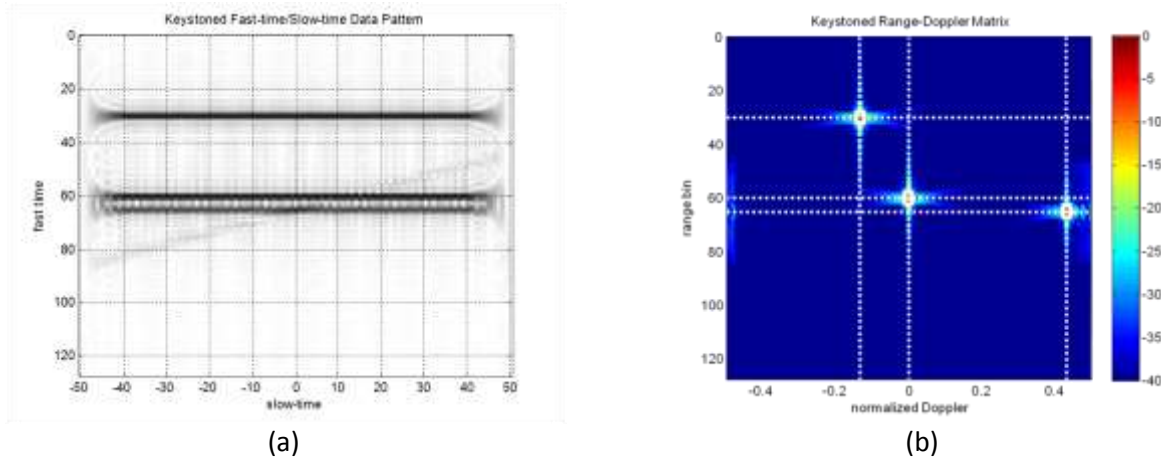


Figure 7. Result of applying the keystone transformation to example of Fig. 6. (a) Range vs. pulse number. (b) Zoom into non-zero portion of the resulting range-Doppler matrix.

## 5 Why "Keystone"?

Why is the process of resampling  $Y_{Rd}(F, m)$  to obtain the new function called a "keystone" transformation? The reason is illustrated in Fig. 8. Part (a) of the figure shows  $|Y_{Rd}(F, m)|$ , the magnitude of the range frequency/slow time spectrum obtained by taking the DFT of the raw ft/st data in the fast-time dimension only. The parameters are those of the three-target example used above. Notice that the spectrum support in fast time is 200 MHz wide, centered on the 1 GHz RF. Part (b) of the figure shows the magnitude of the modified spectrum  $|Y_{Rd\_key}(F, m)|$  resulting from the slow-time interpolation process. Obviously, the spectral support region is no longer a rectangle but is now a keystone shape.<sup>6</sup> This occurs because of the contraction of the slow-time axis for frequencies below  $F_0$  ( $F < 0$ ) and its expansion for frequencies greater than  $F_0$  ( $F > 0$ ) as discussed earlier, giving the keystone-shaped support region seen in Fig. 8b.

It follows that we would expect the slow-time width of  $|Y_{Rd\_key}(F, m)|$  to match that of  $|Y_{Rd}(F, m)|$  at  $F = F_0$  because the slow-time sample spacing is the same at that frequency. Furthermore,  $|Y_{Rd\_key}(F, m)|$  should have wider support than  $|Y_{Rd}(F, m)|$  for frequencies above  $F_0$ . However, the slow-time region of support of  $|Y_{Rd\_key}(F, m)|$  is reduced at each end by about one-half the width of the sinc interpolating function. Furthermore, the slow-time extent of the interpolated data can never exceed that of the original data as discussed earlier. Consequently, the keystone interpolation process

<sup>6</sup> A keystone is the stone at the top of a masonry arch that locks all of the arch stones in place, allowing it to be self supporting and bear weight.



entails a small loss of slow-time support and therefore a small loss of Doppler resolution that increases with interpolating filter size, and must therefore be traded off against the interpolation quality.

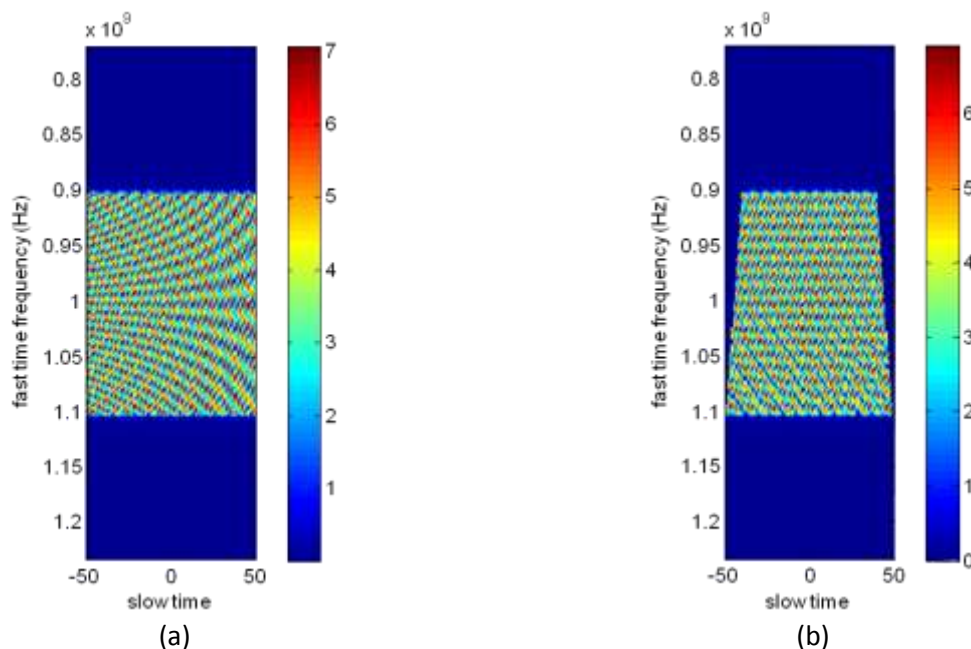
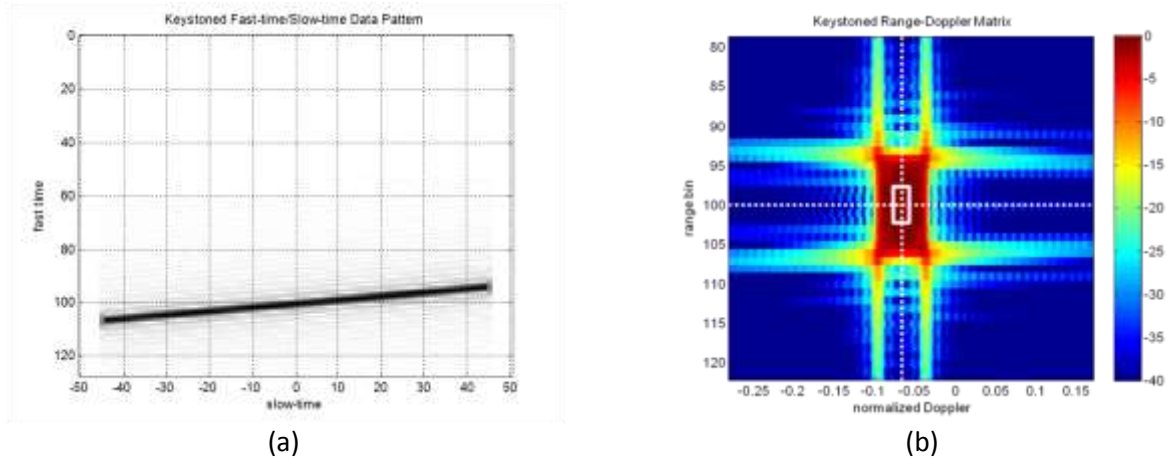


Figure 8. Why it's called a keystone transformation. (a) Magnitude of the range frequency/slow-time spectrum of the raw data. (b) Magnitude of the range frequency/slow-time spectrum after keystone interpolation.

## 6 Effect of Doppler Ambiguity

In all of the examples considered here, the Doppler frequencies of all targets were within the unambiguous Doppler interval for data sampled in slow time at an interval of  $T_{st}$  seconds, namely  $\pm PRF/2 = \pm 1/2T_{st}$  Hz. Figure 9 shows a single-target case where this is not true. All parameters are the same as in the single-target case used earlier, except that the RF is increased by 10× to 10 GHz, thus increasing the Doppler frequency by 10× to  $F_D = 29.33$  kHz. The normalized Doppler shift at 10 GHz is then  $f_D = 2.933$  cycles/sample, which aliases to  $f_{Dn} = -0.0667$  cycles/sample  $= f_D - 3$ . The number of “wraps” of the Doppler (three in this case) is called the Doppler ambiguity number  $N_{amb}$  and is given by  $N_{amb} = f_D - f_{Dn}$ .  $N_{amb}$  can be positive or negative. The raw ft/st data and its range-Doppler spectrum are essentially identical to those of Fig. 3, except that the range-Doppler response is now centered at  $-0.0667$  cycles/sample. Figure 9 shows that the keystone transformation fails to correct the range migration in this case.

归一化多普勒是[-0.5, 0.5]的区间范围，所以2.933这个存在多普勒模糊



**Figure 9. Result of applying the keystone transformation to Doppler-aliased target. See text for parameters. (a) Range vs. pulse number. (b) Zoom into non-zero portion of the resulting range-Doppler matrix.**

Consider the ideal fast-time frequency/slow time spectrum  $Y_{Rd\_ideal}(F, m)$  of Eq. (7). It is sufficient to inspect only the slow-time phase term. Assuming the velocity  $v$  is low enough that it is not ambiguous anywhere in the frequency band  $(F_0 - B/2, F_0 + B/2)$ ,<sup>7</sup> the slow-time phase term can be rewritten in terms of Doppler shift,  $\exp(+j(4\pi/c)F_0 v T_{st} m) = \exp(+j2\pi F_{D0} T_{st} m)$ , where  $F_{D0}$  is the Doppler shift at frequency  $F_0$ . Now suppose that the target velocity is such that the Doppler shift is ambiguous at the slow-time sampling interval  $T_{st}$  and in particular has folded over  $N_{amb}$  times. The slow-time phase term in  $Y_{Rd\_ideal}(F, m)$  becomes  $\exp(+j2\pi [F_{D0} + N_{amb}(1/T_{st})] T_{st} m) = \exp(+j2\pi F_{D0} T_{st} m)$  again; there is no change in the desired result.

Now consider the effect of ambiguous Doppler on the slow-time term of the actual range-frequency/slow time spectrum  $Y_{Rd}(F, \tau)$ :

$$\begin{aligned} \exp\left(+j \frac{4\pi}{c} (F + F_0) v \tau\right) &\Rightarrow \exp\left(+j2\pi \left[\frac{2v}{c} (F + F_0) + N_{amb} \left(\frac{1}{T_{st}}\right)\right] \tau\right) \\ &= \exp\left(+j \frac{4\pi}{c} (F + F_0) v \tau\right) \exp\left(+j2\pi \left(\frac{N_{amb}}{T_{st}}\right) \tau\right) \end{aligned} \quad (14)$$

The rescaling  $\tau \rightarrow \tau'$  to obtain  $Y_{Rd\_key}(F, \tau')$  will, as before, correct the first slow-time phase term to match the ideal result, but will leave an additional phase term due to the Doppler ambiguity:

<sup>7</sup> This assumption allows us to avoid the messiness of the situation where the number of ambiguity wraps is different for different frequencies within the radar bandwidth.

$$\exp\left(+j\frac{4\pi}{c}(F_0 + F)v\tau\right) \exp\left(+j2\pi\left(\frac{N_{amb}}{T_{st}}\right)\tau\right) \xrightarrow{\tau = \left(\frac{F_0}{F_0 + F}\right)\tau'} \exp\left(+j\frac{4\pi}{c}F_0v\tau'\right) \exp\left(+j2\pi N_{amb}\left(\frac{F_0}{F_0 + F}\right)\left(\frac{\tau'}{T_{st}}\right)\right) \quad (15)$$

keystone变换对第一项进行变换处理  
对第二项产生了新问题

This equation shows that the effect of Doppler ambiguity can be removed by multiplying  $Y_{Rd\_key}(F, \tau')$  by the phase function  $\exp\left(-j2\pi N_{amb}\left(\frac{F_0}{(F_0 + F)}\right)\left(\frac{\tau'}{T_{st}}\right)\right)$ , resulting in a focused range-Doppler spectrum for Doppler-ambiguous targets. Taking into account the sampling of the slow-time axis  $\tau' = mT_{st}$ , the required operation to obtain the final result is

$$\hat{Y}_{Rd\_key}(F, m) = Y_{Rd\_key}(F, m) \exp\left(-j2\pi N_{amb}\left(\frac{F_0}{F_0 + F}\right)m\right) \quad (16)$$

终极方案，通过增加模糊数补偿项来消除目标速度模糊的问题

The ambiguity correction requires that  $N_{amb}$  be known, perhaps from tracking data or other sensors, and that it be the same for all targets. If there are multiple targets and the ambiguity numbers are not the same for all targets, only the target(s) having an ambiguity number that matches that used in Eq. (16) will be focused.

Figure 10 illustrates the ambiguous Doppler correction process. The same multitarget example used previously was repeated, but with the RF increased to 10 GHz. The resulting target ambiguity numbers  $-1, 0$ , and  $+4$ . Figure 10a is the range-Doppler plot of the data before the keystone transformation and ambiguity correction. Figure 10b shows the range-Doppler spectrum after the keystone transformation and the correction of Eq. (16) using  $N_{amb} = -1$ . The negative-Doppler target is well-focused. The zero-velocity target is slightly defocused because of processing with the incorrect ambiguity number, although that effect is not very visible in this image. The smearing of the positive-Doppler target is also slightly worsened. Figure 10c repeats the processing with  $N_{amb} = +4$ , appropriate for the positive-Doppler target. That target is now well-focused, while the other two are severely smeared.

The varying amplitude of the target responses in Fig. 10 also shows that the amplitude of the range-Doppler signature of a target varies with the difference between the assumed and correct ambiguity numbers. If the ambiguity number is not known for a given target, it can be estimated by forming the corrected range-Doppler spectrum using several different values, and choosing the one that produces the highest-amplitude peaks. Figure 11 shows the peak amplitude in decibels of the positive-Doppler target as a function of  $N_{amb}$ . The maximum response is obtained when the correct value of  $N_{amb} = 4$  is used. Thus, processing the data with several different values of  $N_{amb}$  can identify the correct value and thus the true velocity.

This ambiguity compensation technique is discussed in both [1] and [2]. In [1], the phase compensation factor is of the same form (after adjusting for notation and a difference in sign in the definition of velocity) given in Eq. (16). In [2], it is given in the form  $\exp\left(+j2\pi N_{amb}\left(F/F_0\right)\left(\tau'/T_{st}\right)\right)$ . The two forms



can be reconciled by noting that, for small fractional bandwidths ( $F \ll F_0$ ),  $F_0/(F + F_0) = 1/(1 + (F/F_0)) \approx 1 - F/F_0$ . Combining this approximation with sampling of the slow-time axis at  $\tau' = mT_{st}$  gives

$$\begin{aligned}\hat{Y}_{Rd\_key}(F, m) &= Y_{Rd\_key}(F, m) \exp \left( -j2\pi N_{amb} \left[ 1 - \left( \frac{F}{F_0} \right) \right] m \right) \\ &= Y_{Rd\_key}(F, m) \exp \left( +j2\pi N_{amb} \left( \frac{F}{F_0} \right) m \right)\end{aligned}\quad (17)$$

The form of Eq. (16) is preferred because the fractional bandwidth may not be particularly small in low-RF, fine-resolution systems. Finally, note that the compensation of Eq. (16) or (17) can be applied before or after the keystone transformation. The code included here performs it afterwards, but is easily modified to perform the ambiguity compensation first and demonstrate this fact.

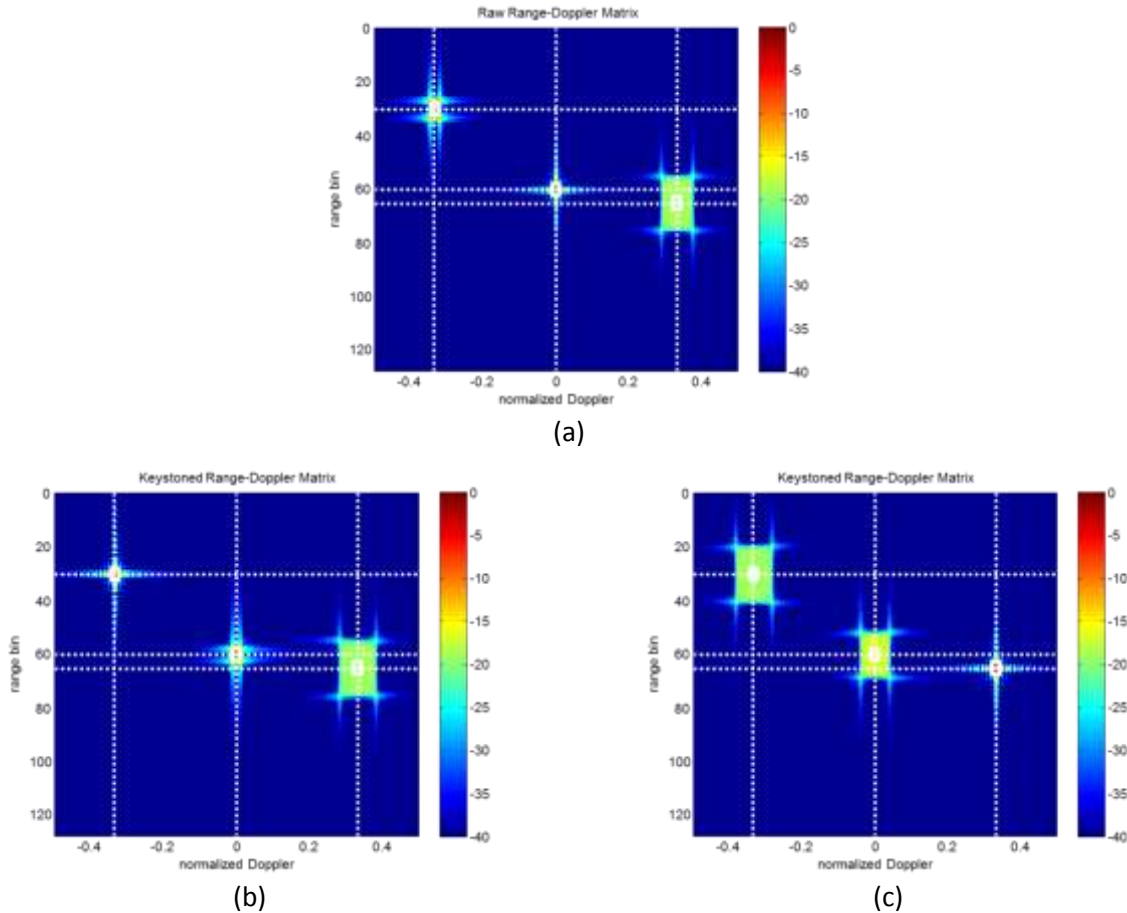


Figure 10. Result of applying keystone processing to Doppler-aliased target. See text for parameters.  
 (a) Before keystone transformation. (b) After keystone transformation with  $N_{amb} = -1$ . (c) After keystone transformation with  $N_{amb} = +4$ .

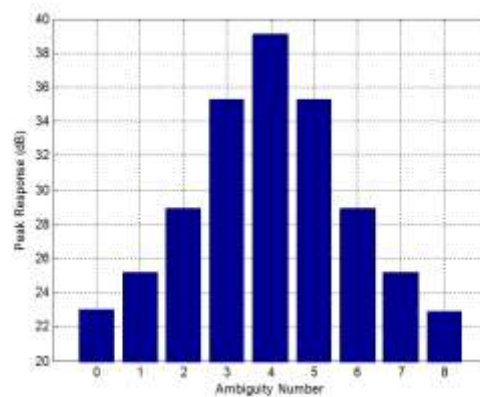


Figure 11. Peak magnitude of the positive-Doppler target response from the example of Fig. 10 as a function of the ambiguity number used in the keystone transformation. The correct ambiguity number of  $N_{amb} = 4$  produces the largest peak response.

## 7 References

- [1] Yang Li, Tao Zeng, Teng Long, and Zheng Wang, "Range Migration Compensation and Doppler Ambiguity Resolution by Keystone Transform", *Proceedings Intl. Conf. on Radar 2006 (CIE 2006)*, pp. 1 – 4, 2006.
- [2] R. P. Perry, R. C. DiPietro, and R. Fante, "Coherent Integration With Range Migration Using Keystone Formatting", *Proceedings 2007 IEEE Radar Conference*, pp. 863 – 868, 2007.
- [3] M. A. Richards, *Fundamentals of Radar Signal Processing*, second edition. McGraw-Hill, 2014.
- [4] A. V. Oppenheim and R. W. Schaffer, *Discrete-Time Signal Processing*, third edition. Prentice-Hall, 2009.

## 8 Demonstration MATLAB® Code

Following are the two scripts used to generate the examples in this memo. The script `keystone.m` was used to generate the single target examples, while `keystone_multitarget` was used for the three-target example. Also included is the script `sinc_interp.m` used for the keystone interpolation. The scripts `hline.m` and `vline.m` used for some plot markings are available from the MATLAB® File Exchange at <http://www.mathworks.com/matlabcentral/fileexchange/>.

## keystone.m

```
% keystone
%
% Demo of keystone formatting for correcting range-Doppler
% measurements for range migration.
%
% This code closely follows the equations in the tech memo "The Keystone
% Transformation for Correcting Range Migration in Range-Doppler
% Processing" by Mark A. Richards, Mar. 2014, available at www.radarsp.com.
%
% Mark Richards
%
% March 2014

clear all
close all

c = 3e8; % speed of light

%%%%%%%%%%%%%%%%%%%%%%%%%%%%%%%%%%%%%%%%%%%%%%%%%%%%%%%%%%%%%%%%%%%%%%%%%%%%%%
% USER INPUT SECTION
%%%%%%%%%%%%%%%%%%%%%%%%%%%%%%%%%%%%%%%%%%%%%%%%%%%%%%%%%%%%%%%%%%%%%%%%%%%%%%
L = 128; % fast time dimension, samples
M = 101; % slow-time dimension, samples; keep it odd.

% K_L and K_M must be even to avoid labeling problems later
K_L = 2^(nextpow2(128)+1); % fast-time DFT size for interpolation and shifting
K_M = 2^(nextpow2(512)+1); % slow-time DFT size

% Lref is the range bin # of the target, on a 0:L-1 scale, at the center of
% the CPI (middle pulse)
% Lref = round(L/2); % puts target at middle range bin on the middle pulse
Lref = 100;

F0 = 1000e6; % RF (Hz)
B = 200e6; % waveform bandwidth (Hz)

v = 440; % velocity in m/s towards the radar

% sampling intervals and rates
Fsft = 2.3*B;

PRF = 10e3;

% Order of sinc interpolating filter
Nsinc = 11;

%%%%%%%%%%%%%%%%%%%%%%%%%%%%%%%%%%%%%%%%%%%%%%%%%%%%%%%%%%%%%%%%%%%%%%%%%%%%%%
% END USER INPUT SECTION
%%%%%%%%%%%%%%%%%%%%%%%%%%%%%%%%%%%%%%%%%%%%%%%%%%%%%%%%%%%%%%%%%%%%%%%%%%%%%%

% Some derived parameters
m_end = (M-1)/2;
ms = (-m_end:m_end); % slow time index labels
Fd = 2*v*F0/c; % Doppler shift, Hz
Tft = 1/Fsft; % fast time sampling interval
dr = c*Tft/2; % range bin spacing
Tst = 1/PRF; % slow-time sampling interval (PRI)
```

```
Dfd = 1/M; % Rayleigh Doppler resolution in cycles/sample
Drb = (1/B)/Tft; % Rayleigh fast-time resolution in range bins

if (PRF < Fd/2)
    fprintf('\nWarning: PRF < Fd/2. PRF = %g, Fd = %g.\n', PRF, Fd)
end

% Compute and report total range migration over the CPI in range bins
RM = v*Tst/dr; % amount of range migration per pulse in range bins
RMtot = M*RM; % total range migration over the dwell, in range bins
fprintf('\nTotal range migration = %g m = %g range bins.\n', RMtot*dr, RMtot)

if ( (floor(Lref-RMtot/2) < 0) || (ceil(Lref+RMtot/2) > L-1) )
    fprintf(['\nWarning: Target will migrate out of range.', ...
        'RMtot = %g range bins, Lref = %g, L = %g range bins.\n'], RMtot, Lref, L)
end

% Compute normalized Doppler frequency and wrap it
fd = Fd*Tst;
fdn = mod(fd + 0.5, 1) - 0.5; % alias it back into [-0.5, +0.5]
amb_num = round(fd - fdn); % number of Doppler wraps

% Define corners of a box centered on the expected target coordinates, and
% one Rayleigh width wide in each direction and each dimension (i.e., a
% null-to-null resolution box for a well-formed sinc spectrum). Will use
% this to draw such a resolution box on some of the figures.
L1 = Lref - Drb;
L2 = Lref + Drb;
fd1 = fdn - Dfd;
fd2 = fdn + Dfd;

%%%%%%%%%%%%%%%%%%%%%%%%%%%%%%%%%%%%%%%%%%%%%%%%%%%%%%%%%%%%%%%%%%%%%%%%
% Create synthetic data. First compute pulse-to-pulse phase shift. Then set
% up a matrix. Loop over pulses, computing current range. The range
% profile of the compressed data for a single pulse is assumed to be a sinc
% function with a zero spacing equal to 1/B seconds, and a phase shift of
% the usual  $-(4\pi F_0/c)R$ , where  $R = R_{ref} - vT_{st}m$  and  $m$  = pulse number.
% Don't worry about amplitude. Also don't bother with the
%  $-(4\pi F_0/c)R_{ref}$  phase term, it is the same for all pulses.

del_phi =  $-4\pi(F_0/c)vT_{st}$ ; % pulse-to-pulse phase increment due to range change
y = zeros(L, M);

for m = 1:M
    mm = ms(m); % counts from  $-(M-1)/2$  to  $+(M-1)/2$ 
    y(:, m) = exp(-1i*del_phi*mm)*sinc( B*Tft*((0:L-1)-Lref+v*Tst*mm/dr) );
end

% Now examine the data. Then compute the range-Doppler matrix with a
% slow-time DFT and look at that.

figure
imagesc(ms, 0:L-1, abs(y))
grid
colormap(flipud(gray))
xlabel('pulse number')
ylabel('range bin')
title('Raw Fast-time/Slow-time Data Pattern')

Y_rD = fft(y, K_M, 2);
Y_rD = fftshift(Y_rD, 2);
Y_rD_db = db(abs(Y_rD), 'voltage');
```

```

Y_rD_dB = Y_rD_dB - max(Y_rD_dB(:)); % normalize to 0 dB max
Y_rD_dB(:) = max(-40,Y_rD_dB(:)); % limit dynamic range for plot purposes

fD = (-K_M/2:K_M/2-1)/K_M; % this only works correctly if K_M is even

% figure
% mesh(fD,0:L-1,Y_rD_dB)
% xlabel('normalized Doppler')
% ylabel('range bin')
% title('Raw Range-Doppler Matrix')

figure
imagesc(fD,0:L-1,Y_rD_dB)
hline(Lref,':w'); vline(fdn,':w') % mark the correct spectrum center
line([fd1 fd1 fd2 fd2 fd1],[L1 L2 L2 L1 L1],'Color','w','LineWidth',2) % resolution
box
title(['Rng Migration = ',num2str(RMtot),...
      ' bins over CPI; Normalized Doppler = ',num2str(fdn),' cyc/samp'])
xlabel('normalized Doppler')
ylabel('range bin')
colorbar
shg

% It is convenient to look at the fast time DFT of the raw data as well. We
% will need this product as the starting point for keystoneing a little
% further down. Apply a fast-time DFT. fftshift in fast-time freq dimension
% to center the origin. This will be the frequency corresponding to F0.
% Also work out axis label in Hz.
Y_Rd = fftshift(fft(y,K_L,1),1);

F1 = (-K_L/2:K_L/2-1)/K_L*Fsft;

figure
subplot(1,2,1)
imagesc(ms,F0+F1,abs(Y_Rd))
xlabel('slow time')
ylabel('fast time frequency (Hz)')
title('Magnitude after fast-time FT')
colorbar

subplot(1,2,2)
imagesc(ms,F0+F1,angle(Y_Rd))
xlabel('slow time')
ylabel('fast time frequency (Hz)')
title('Unwrapped phase after fast-time FT')
colorbar

%%%%%%%%%%%%%%%%%%%%%%%%%%%%%%%%%%%%%%%%%%%%%%%%%%%%%%%%%%%%%%%%%%%%%%%%
% Now do compensation by explicit shifting and interpolation in range for
% each pulse to see that that does indeed work (for a single target with
% known velocity) and verify formulas
%
yc = zeros(size(y)); % this will be the compensated fast-time/slow-time data
wl = 2*pi*(-K_L/2:K_L/2-1)/K_L; % normalized fast time freq in radians/sample

for m = 1:M % loop over pulses
    mm = ms(m); % counts from -(M-1)/2 to +(M-1)/2
    Lm = v*Tst*mm/dr; % # of range bins of shift needed
    Y_shift = fftshift(fft(y(:,m),K_L)).*exp(-1i*wl*Lm);
    y_shift_temp = ifft(ifftshift(Y_shift));
    y_shift(:,m) = y_shift_temp(1:L);
end % of loop over pulses

```

```
figure
imagesc(ms,0:L-1,abs(y_shift))
colormap(flipud(gray))
grid
xlabel('pulse number')
ylabel('range bin')
title('Data Pattern after Compensation by Shifting')

Y_shift = fft(y_shift,K_M,2);
Y_shift = fftshift(Y_shift,2);
Y_shift_dB = db(abs(Y_shift),'voltage');
Y_shift_dB = Y_shift_dB - max(Y_shift_dB(:)); % normalize to 0 dB max
Y_shift_dB(:) = max(-40,Y_shift_dB(:)); % limit to 40 dB range

% figure
% mesh(fD,0:L-1,Y_shift_dB)
% xlabel('normalized Doppler')
% ylabel('range bin')
% title('Range-Doppler Matrix after Compensation by Shifting')

figure
imagesc(fD,0:L-1,Y_shift_dB)
hline(Lref,'w'); vline(fdn,'w') % mark the correct spectrum center
line([fd1 fd1 fd2 fd2 fd1],[L1 L2 L2 L1 L1],'Color','w','LineWidth',2) % resolution
box
xlabel('normalized Doppler')
ylabel('range bin')
title('Range-Doppler Matrix after Compensation by Shifting')
shg
colorbar

% Let's also look at the fast-time DFT of this data. It will show what
% we're trying to get to with the keystoneing in the next section.

Y_Rd_shift = fftshift(fft(y_shift,K_L,1),1);

figure
subplot(1,2,1)
imagesc(ms,F0+F1,abs(Y_Rd_shift))
xlabel('slow time')
ylabel('fast time frequency (Hz)')
title('Magnitude after fast-time FT')
colorbar

subplot(1,2,2)
imagesc(ms,F0+F1,angle(Y_Rd_shift))
xlabel('slow time')
ylabel('fast time frequency (Hz)')
title('Unwrapped phase after fast-time FT')
colorbar

%%%%%%%%%%%%%%%%%%%%%%%%%%%%%%%%%%%%%%%%%%%%%%%%%%%%%%%%%%%%%%%%%%%%%%%%
% Now start over and correct by keystoneing. Begin with Y_Rd, i.e. data
% DFT'ed in fast time but not in slow time. For each fast-time frequency
% bin, compute a new, interpolated slow-time sequence. Use the existing
% sinc_interp function for bandlimited, Hamming-weighted interpolation to
% do the work.

Y_Rd_key = zeros(size(Y_Rd));

for k = 1:K_L
```

```

[y_temp,mm_i] = sinc_interp(Y_Rd(k,:),ms,(F0/(F0+F1(k)))*ms,Nsinc,1);
% y_temp = interp1(ms,Y_Rd(k,:), (F0/(F0+F1(k)))*ms,'spline');
% Mi will always be odd the way I'm setting up the problem. Also, Mi <= M.
Mi = length(y_temp);
dM = M - Mi; % dM will be even so long as M and Mi are odd
Y_Rd_key(k,1+dM/2:1+dM/2+Mi-1) = y_temp; % center the interpolated data in slow
time
end

% Now correct the modified spectrum for the ambiguity number of the
% Doppler. This code uses the ambiguity number of the first target. So if
% the other targets have a different ambiguity number it won't be correct
% for them. The first version of the correction corresponds to the Li et al
% paper and is consistent with my memo. The second (commented out)
% corresponds to the Perry et al paper and can be obtained from the first
% using a binomial expansion approximation to (F0/(F0+F1)). Either one
% works if done either after the keystone correction, as is done here, or
% before.
for mp = 1:M
    for k = 1:K_L
        mmp = ms(mp); % counts from -(M-1)/2 to +(M-1)/2
        Y_Rd_key(k,mp) = Y_Rd_key(k,mp)*exp(1i*2*pi*amb_num(1)*mmp*(F0/(F0+F1(k))));
% Y_Rd_key(k,mp) = Y_Rd_key(k,mp)*exp(-1i*2*pi*amb_num(1)*mmp*(F1(k)/F0));
    end
end

% Now IDFT in fast-time and DFT in slow time to get range-Doppler matrix
y_temp_key = ifft( ifftshift(Y_Rd_key,1),K_L,1 );
y_rd_key = y_temp_key(1:L,:);
Y_rD_key = fftshift( fft(y_rd_key,K_M,2),2 );

Y_rD_key_dB = db(abs(Y_rD_key),'voltage');
Y_rD_key_dB = Y_rD_key_dB - max(Y_rD_key_dB(:)); % normalize to 0 dB max
Y_rD_key_dB(:) = max(-40,Y_rD_key_dB(:)); % limit to 40 dB range

figure
imagesc(ms,0:L-1,abs(y_rd_key))
grid
colormap(flipud(gray))
xlabel('slow-time')
ylabel('fast time')
title('Keystoned Fast-time/Slow-time Data Pattern')

% figure
% mesh(fD,0:L-1,Y_rD_key_dB)
% xlabel('normalized Doppler')
% ylabel('fast time')
% title('Keystoned Range-Doppler Matrix')

figure
imagesc(fD,0:L-1,Y_rD_key_dB)
hline(Lref,'w'); vline(fdn,'w') % mark the correct spectrum center
line([fd1 fd1 fd2 fd2 fd1],[L1 L2 L2 L1 L1],'Color','w','LineWidth',2) % resolution
box
xlabel('normalized Doppler')
ylabel('range bin')
title('Keystoned Range-Doppler Matrix')
shg
colorbar

figure
subplot(1,2,1)

```



```
imagesc(ms,F0+F1,abs(Y_Rd_key))
xlabel('slow time')
ylabel('fast time frequency (Hz)')
title('Magnitude after interpolation')
colorbar

subplot(1,2,2)
imagesc(ms,F0+F1,angle(Y_Rd_key))
xlabel('slow time')
ylabel('fast time frequency (Hz)')
title('Unwrapped phase after interpolation')
colorbar
```

## keystone\_multitarget.m

```
% keystone_multitarget
%
% Demo of keystone formatting for correcting range-Doppler
% measurements for range migration, with multiple targets at different
% speeds.
%
% This code closely follows the equations in the tech memo "The Keystone
% Transformation for Correcting Range Migration in Range-Doppler
% Processing" by Mark A. Richards, Mar. 2014, available at www.radarsp.com.
%
% Mark Richards
%
% March 2014

clear all
close all

c = 3e8; % speed of light

%%%%%%%%%%%%%%%%%%%%%%%%%%%%%%%%%%%%%%%%%%%%%%%%%%%%%%%%%%%%%%%%%%%%%%%%%%%%%%
% USER INPUT SECTION
%%%%%%%%%%%%%%%%%%%%%%%%%%%%%%%%%%%%%%%%%%%%%%%%%%%%%%%%%%%%%%%%%%%%%%%%%%%%%%
L = 128; % fast time dimension, samples
M = 101; % slow-time dimension, samples; keep it odd.

% K_L and K_M must be even to avoid labeling problems later
K_L = 2^(nextpow2(128)+1); % fast-time DFT size for interpolation and shifting
K_M = 2^(nextpow2(512)+1); % slow-time DFT size

Ntgt = 3;
v = [-200,0,650]; % velocities in m/s towards the radar
% Lref is the range bin # of the targets, on a 0:L-1 scale, at the center of
% the CPI (middle pulse)
% Lref = round(L/2); % puts target at middle range bin on the middle pulse
Lref = [30,60,65];

F0 = 10000e6; % RF (Hz)
B = 200e6; % waveform bandwidth (Hz)

% sampling intervals and rates
Fsft = 2.3*B;

PRF = 10e3;
```

```
% Order of sinc interpolating filter
Nsinc = 11;

%%%%%%%%%%%%%%%%%%%%%%%%%%%%%%%%%%%%%%%%%%%%%%%%%%%%%%%%%%%%%%%%%%%%%%%%
% END USER INPUT SECTION
%%%%%%%%%%%%%%%%%%%%%%%%%%%%%%%%%%%%%%%%%%%%%%%%%%%%%%%%%%%%%%%%%%%%%%%%

% Some derived parameters
m_end = (M-1)/2;
ms = (-m_end:m_end); % slow time index labels
Fd = 2*v*F0/c; % Doppler shifts, Hz
Tft = 1/Fsft; % fast time sampling interval
dr = c*Tft/2; % range bin spacing
Tst = 1/PRF; % slow-time sampling interval (PRI)
Dfd = 1/M; % Rayleigh Doppler resolution in cycles/sample
Drb = (1/B)/Tft; % Rayleigh fast-time resolution in range bins

if (PRF < Fd/2)
    fprintf('\nWarning: PRF < Fd/2. PRF = %g, Fd = %g.\n',PRF,Fd)
end

% Compute and report total range migration over the CPI in range bins
RM = v*Tst/dr; % amount of range migration per pulse in range bins
RMtot = M*RM % total range migration over the dwell, in range bins

% Compute normalized Doppler frequencies and wrap them
fd = Fd*Tst
fdn = mod(fd + 0.5,1) - 0.5 % alias back into [-0.5,+0.5]
amb_num = round(fd - fdn); % number of Doppler wraps

% Define corners of a box centered on the expected target coordinates, and
% one Rayleigh width wide in each direction and each dimension (i.e., a
% null-to-null resolution box for a well-formed sinc spectrum). Will use
% this to draw such a resolution box on some of the figures.
L1 = Lref - Drb;
L2 = Lref + Drb;
fd1 = fdn - Dfd;
fd2 = fdn + Dfd;

%%%%%%%%%%%%%%%%%%%%%%%%%%%%%%%%%%%%%%%%%%%%%%%%%%%%%%%%%%%%%%%%%%%%%%%%
% Create synthetic data. First compute pulse-to-pulse phase shift. Then set
% up a matrix. Loop over pulses, computing current range. The range
% profile of the compressed data for a single pulse is assumed to be a sinc
% function with a zero spacing equal to 1/B seconds, and a phase shift of
% the usual  $-(4\pi F_0/c)*R$ , where  $R = Rref - v*Tst*m$  and  $m$  = pulse number.
% Don't worry about amplitude. Also don't bother with the
%  $-(4\pi F_0/c)*Rref$  phase term, it is the same for all pulses.

y = zeros(L,M);

for t = 1:Ntgt
    del_phi = -4*pi*(F0/c)*v(t)*Tst; % pulse-to-pulse phase increment due to range
    change

        for m = 1:M
            mm = ms(m); % counts from  $-(M-1)/2$  to  $+(M-1)/2$ 
            y(:,m) = y(:,m) + exp(-1i*del_phi*mm)*sinc( B*Tft*((0:L-1)'+
            Lref(t)+v(t)*Tst*mm/dr) );
        end
    end % of loop over targets
```

```
% Now examine the data.  Then compute the range-Doppler matrix with a
% slow-time DFT and look at that.

figure
imagesc(ms,0:L-1,abs(y))
grid
colormap(flipud(gray))
xlabel('pulse number')
ylabel('range bin')
title('Raw Fast-time/Slow-time Data Pattern')

Y_rD = fft(y,K_M,2);
Y_rD = fftshift(Y_rD,2);
Y_rD_dB = db(abs(Y_rD),'voltage');
Y_rD_dB = Y_rD_dB - max(Y_rD_dB(:)); % normalize to 0 dB max
Y_rD_dB(:) = max(-40,Y_rD_dB(:)); % limit dynamic range for plot purposes

fD = (-K_M/2:K_M/2-1)/K_M; % this only works correctly if K_M is even

% figure
% mesh(fD,0:L-1,Y_rD_dB)
% xlabel('normalized Doppler')
% ylabel('range bin')
% title('Raw Range-Doppler Matrix')

figure
imagesc(fD,0:L-1,Y_rD_dB)
title('Raw Range-Doppler Matrix')
xlabel('normalized Doppler')
ylabel('range bin')
for t = 1:Ntgt
    hline(Lref(t),':w'); vline(fdn(t),':w') % mark the correct spectrum center
    line([fd1(t) fd1(t) fd2(t) fd2(t) fd1(t)], ...
         [L1(t) L2(t) L2(t) L1(t) L1(t)], 'Color','w','LineWidth',2) % resolution box
end
colorbar
shg

% It is convenient to look at the fast time DFT of the raw data as well. We
% will need this product as the starting point for keystoneing a little
% further down. Apply a fast-time DFT. fftshift in fast-time freq dimension
% to center the origin. This will be the frequency corresponding to F0.
% Also work out axis label in Hz.
Y_Rd = fftshift(fft(y,K_L,1),1);

F1 = (-K_L/2:K_L/2-1)/K_L*Fsft;

figure
subplot(1,2,1)
imagesc(ms,F0+F1,abs(Y_Rd))
xlabel('slow time')
ylabel('fast time frequency (Hz)')
title('Magnitude after fast-time FT')
colorbar

subplot(1,2,2)
imagesc(ms,F0+F1,angle(Y_Rd))
xlabel('slow time')
ylabel('fast time frequency (Hz)')
title('Unwrapped phase after fast-time FT')
colorbar
```

```

%%%%%%%%%%%%%%%%%%%%%%%%%%%%%%%%%%%%%%%%%%%%%%%%%%%%%%%%%%%%%%%%%%%%%%%%
% Now start over and correct by keystoning. Begin with Y_Rd, i.e. data
% DFT'ed in fast time but not in slow time. For each fast-time frequency
% bin, compute a new, interpolated slow-time sequence. Use the existing
% sinc_interp function for bandlimited, Hamming-weighted interpolation to
% do the work.

Y_Rd_key = zeros(size(Y_Rd));

for k = 1:K_L
    [y_temp,mm_i] = sinc_interp(Y_Rd(k,:),ms,(F0/(F0+F1(k)))*ms,Nsinc,1);
    % y_temp = interp1(ms,Y_Rd(k,:), (F0/(F0+F1(k)))*ms,'spline');
    % Mi will always be odd the way I'm setting up the problem. Also, Mi <= M.
    Mi = length(y_temp);
    dM = M - Mi; % dM will be even so long as M and Mi are odd
    Y_Rd_key(k,1+dM/2:1+dM/2+Mi-1) = y_temp; % center the interpolated data in slow
time
end

% Now correct the modified spectrum for the ambiguity number of the
% Doppler. This code uses the ambiguity number of the first target. So if
% the other targets have a different ambiguity number it won't be correct
% for them. The first version of the correction corresponds to the Li et al
% paper and is consistent with my memo. The second (commented out)
% corresponds to the Perry et al paper and can be obtained from the first
% using a binomial expansion approximation to (F0/(F0+F1)). Either one
% works if done either after the keystone correction, as is done here, or
% before.
for mp = 1:M
    for k = 1:K_L
        mmp = ms(mp); % counts from -(M-1)/2 to +(M-1)/2
        Y_Rd_key(k,mp) = Y_Rd_key(k,mp)*exp(1i*2*pi*amb_num(1)*mmp*(F0/(F0+F1(k))));
        % Y_Rd_key(k,mp) = Y_Rd_key(k,mp)*exp(-1i*2*pi*amb_num(1)*mmp*(F1(k)/F0));
    end
end

% Now IDFT in fast-time and DFT in slow time to get range-Doppler matrix
y_temp_key = ifft( ifftshift(Y_Rd_key,1),K_L,1 );
y_rd_key = y_temp_key(1:L,:);
Y_rD_key = fftshift( fft(y_rd_key,K_M,2),2 );

Y_rD_key_dB = db(abs(Y_rD_key),'voltage');
Y_rD_key_dB = Y_rD_key_dB - max(Y_rD_key_dB(:)); % normalize to 0 dB max
Y_rD_key_dB(:) = max(-40,Y_rD_key_dB(:)); % limit to 40 dB range

figure
imagesc(ms,0:L-1,abs(y_rd_key))
grid
colormap(flipud(gray))
xlabel('slow-time')
ylabel('fast time')
title('Keystoned Fast-time/Slow-time Data Pattern')

% figure
% mesh(fD,0:L-1,Y_rD_key_dB)
% xlabel('normalized Doppler')
% ylabel('fast time')
% title('Keystoned Range-Doppler Matrix')

figure
imagesc(fD,0:L-1,Y_rD_key_dB)

```

```
xlabel('normalized Doppler')
ylabel('range bin')
title('Keystoned Range-Doppler Matrix')
for t = 1:Ntgt
    hline(Lref(t),':w'); vline(fdn(t),':w') % mark the correct spectrum center
    line([fd1(t) fd1(t) fd2(t) fd2(t) fd1(t)], [L1(t) L2(t) L2(t) L1(t)
L1(t)], 'Color','w', 'LineWidth',2) % resolution box
end
colorbar
shg

figure
subplot(1,2,1)
imagesc(ms,F0+F1,abs(Y_Rd_key))
xlabel('slow time')
ylabel('fast time frequency (Hz)')
title('Magnitude after interpolation')
colorbar

subplot(1,2,2)
imagesc(ms,F0+F1,angle(Y_Rd_key))
xlabel('slow time')
ylabel('fast time frequency (Hz)')
title('Unwrapped phase after interpolation')
colorbar
```

### **sinc\_interp.m**

```
function [out,x_out] = sinc_interp(in,x_in,x_new,N,win)
%
% sinc_interp
%
% Sinc-based (band-limited) interpolation.
%
% INPUTS
%   in = data sequence to be interpolated
%   x_in = vector of sample locations corresponding to data samples of 'in'.
%           Must be uniformly spaced at some interval dx_in. Must be same
%           length as 'in'.
%   x_new = vector of desired sample locations. Must be uniformly spaced at
%           some interval dx_out.
%   N = order of interpolating sinc, in units of max(dx_in,dx_out).
%       Must be odd.
%   win = 1 if Hamming window applied to interpolation kernel, otherwise no
%         window. (win=1 is recommended.)
%
% OUTPUTS
%   out = interpolated data sequence corresponding to sample locations in
%         x_out.
%   x_out = sample locations of output vector. This will be a subset of the
%           locations in x_new; relative span of x_new and x_in, and filter
%           end effects, may limit x_out to not include some of the values in
%           x_new.
%
% Mark A. Richards
% February 2007
%
if (mod(N,2) ~= 1)
    disp(' ')
    disp(' ** Error: sinc_interp : filter order not odd.')
```

```

    disp([' ** Filter order input = ',int2str(N)])
    disp(' ')
    return
end
Nhalf = (N-1)/2;

d_in = x_in(2) - x_in(1);
d_out = x_new(2) - x_new(1);

% Now figure out interpolating filter impulse response in continuous time.
% This will be a sinc function, possibly windowed. Bandwidth of the sinc
% LPF frequency response is based on the larger sampling interval of the
% two grids. Specifically, the unwindowed impulse response is  $h(x) = \sin(\pi x / \text{del}) / (\pi x)$  and  $\text{dt} = \max(\text{dt1}, \text{dt2})$ . To add to this, we specify
% how many sample increments we will go out on the tails, where 1 increment
% is dt; and then we also apply a hamming window of the same length. The
% Hamming formula in continuous time is  $w(t) = 0.54 + 0.46 \cos(\pi t / \text{dt})$ .
del = max(d_in, d_out);

% find the values within x_new that can be successfully interpolated from the
% values available in x_in, i.e. where end effects won't kill us.
% x_in
% x_new
% Nhalf
% x_new(1)-Nhalf*del
% x_in(1)
% x_new(end)+Nhalf*del
% x_in(end)

index = find( (x_new-Nhalf*del >= x_in(1) ) & ...
    (x_new+Nhalf*del <= x_in(end)) );
if (isempty(index))
    disp(' ')
    disp(' ** Error: sinc_interp : Requested output samples cannot be interpolated')
    disp(' ')
    return
end
x_out = x_new(index);
out = zeros(size(x_out));

% step through the output samples one at a time, interpolating a value for
% each one from the input samples.
for k = 1:length(x_out)
    % first find the span of the interpolating filter on the x axis
    x_current = x_out(k);
    x_low = x_current - Nhalf*del;
    x_high = x_current + Nhalf*del;
    % compute the *relative* position of each input sample within this span
    % compared to the current output sample location; these will be the
    % values at which the interpolating kernel filter response will be
    % needed.
    index_rel = find( (x_in >= x_low) & ...
        (x_in <= x_high) );
    x_rel = x_in(index_rel) - x_current;

    % Now compute and apply the sinc weights. First fix any spots where
    % x_rel = 0; these will cause the sinc function to be undefined. Then
    % add in the window, if used, and apply to the data to compute the
    % output point.
    trouble = find(x_rel==0);
    if (~isempty(trouble))

```

```
        x_rel(trouble) = x_rel(trouble)+eps; % this will prevent division by zero
    end
    h = (sin(pi*x_rel/del)/pi./x_rel);
    w = ones(size(h));
    if (win == 1)
        w = 0.54 + 0.46*cos(pi*x_rel/del/(Nhalf+1));
        h = h.*w;
    end
    h = h/sum(h);
    out(k) = sum( in(index_rel).*h);
end

% % Diagnostic figures showing a sample of sinc kernel and Hamming weights,
% % original and interpolated waveforms, and spectra of same.
% figure
% stem(x_rel,[h;w]')
% figure
% plot(x_in,real(in));
% title('Continuous Sinc Interpolation')
% hold on
% plot(x_out,real(out),'r');
% hold off
%
% % plot before-and-after spectra for a quality check. Note that different
% % sampling rates mean I need to use different frequency scales, and they
% % can't be normalized frequency.
% % figure
% Nfft = 2^(ceil(log2(max(length(x_out),length(x_in))))+2);
% X_in = d_in*fft(in,Nfft);
% f_in = (1/d_in)*((0:Nfft-1)/Nfft-0.5);
% X_out = d_out*fft(out,Nfft);
% f_out = (1/d_out)*((0:Nfft-1)/Nfft-0.5);
% % plot(f_in,abs(fftshift(X_in)))
% % title('Continuous Sinc Interpolation')
% % hold on
% % plot(f_out,abs(fftshift(X_out)),'r')
% % grid
% % hold off
% figure
% plot(f_in,db(abs(fftshift(X_in)),'voltage'))
% title('Continuous Sinc Interpolation')
% hold on
% plot(f_out,db(abs(fftshift(X_out)),'voltage'),'r')
% grid
% hold off
% pause
```